RESEARCH ARTICLE

Diagnosis of Alzheimer's disease with Electroencephalography in a differential framework

Nesma Houmani[1]*, François Vialatte[2,3], Esteve Gallego-Jutglà[4], Gérard Dreyfus[3], Vi-Huong Nguyen-Michel[5], Jean Mariani[5,6,7], Kiyoka Kinugawa[5,6,7]

1 SAMOVAR, Télécom SudParis, CNRS, Université Paris-Saclay, 9 rue Charles Fourier EVRY, France, 2 UMR CNRS 8249 Brain Plasticity Laboratory, Paris, France, 3 ESPCI Paris, PSL Research University, Paris, France, 4 Data and Signal Processing Research Group, U Science Tech, University of Vic–Central University of Catalonia, Vic, Catalonia, Spain, 5 AP-HP, DHU FAST, GH Pitié-Salpêtrière-Charles Foix, Functional Exploration Unit of older patients, Ivry-sur-Seine, France, 6 Sorbonne Universités, UPMC Univ Paris 06, UMR 8256, Biological Adaptation and Ageing, Paris, France, 7 CNRS, UMR 8256, Biological Adaptation and Ageing, Paris, France

* nesma.houmani@telecom-sudparis.eu

Abstract

This study addresses the problem of Alzheimer's disease (AD) diagnosis with Electroencephalography (EEG). The use of EEG as a tool for AD diagnosis has been widely studied by comparing EEG signals of AD patients only to those of healthy subjects. By contrast, we perform automated EEG diagnosis in a differential diagnosis context using a new database, acquired in clinical conditions, which contains EEG data of 169 patients: subjective cognitive impairment (SCI) patients, mild cognitive impairment (MCI) patients, possible Alzheimer's disease (AD) patients, and patients with other pathologies. We show that two EEG features, namely epoch-based entropy (a measure of signal complexity) and bump modeling (a measure of synchrony) are sufficient for efficient discrimination between these groups. We studied the performance of our methodology for the automatic discrimination of possible AD patients from SCI patients and from patients with MCI or other pathologies. A classification accuracy of 91.6% (specificity = 100%, sensitivity = 87.8%) was obtained when discriminating SCI patients from possible AD patients and 81.8% to 88.8% accuracy was obtained for the 3-class classification of SCI, possible AD and other patients.

Introduction

Dementia is a major public health issue worldwide. The impact on aging population grows at an alarming rate: the number of people living with dementia today is estimated at 46.8 millions, and expected to double by 2030 and triple by 2050 [1]. Alzheimer's disease is the most common form of neurodegenerative dementia, accounting for up to 75% of all dementia cases; it is a growing challenge to public health and the health care systems.

Alzheimer's disease (AD) is an irreversible neurodegenerative disease characterized by a decline in memory, language and other cognitive functions that affect a person's ability to

Abbreviations: AD, Alzheimer's disease; BM, Bump models; EpEn, Epoch-based entropy; HMM, Hidden Markov Model; MCI, Mild Cognitive Impairment; aMCI, amnestic Mild Cognitive Impairment; MMSE, Mini Mental Status Examination; OFR, Orthogonal Forward Regression; Other, patients with MCI or other pathologies; SCI, subjective cognitive impairment; SVM, Support Vector Machine.

perform daily activities. The evolution of the disease frequently follows five stages. The "preclinical" stage is asymptomatic, but the brain lesions of Alzheimer's disease are present. In the subgroup of preclinical stage, the concept of subjective cognitive decline/impairment (SCI) has been proposed recently, defined by a self-experienced persistent decline in cognitive capacity in comparison with a previously normal status and with normal age-, gender- and education-adjusted performance on cognitive tests [2]. These subjective complaints are considered as a risk factor for AD [3]. In the second stage ("Mild Cognitive Impairment"–MCI), patients have some memory impairments, but maintain their functional capacities [4,5]; 6% to 25% of MCI patients later develop Alzheimer's dementia. Then, in the "Mild" stage of Alzheimer's dementia (MMSE>20), cognitive deficits are notable such as memory and learning impairments, which become more severe in the "Moderate AD" stage (MMSE between 10 and 20). In the final "severe" stage of the disease, almost all cognitive and motor functions are deeply deteriorated and patients are completely dependent on caregivers [6]. The average duration of survival of Alzheimer's disease patients is 5–8 years after clinical diagnosis [7,8]. Currently, no known medication exists for curing this pathology, but some therapeutic treatments at the early stage might delay the evolution of the disease [9,10]. Therefore, an early diagnosis of Alzheimer's disease in MCI and Mild AD stages becomes an important issue for the scientific and medical community.

Medical diagnosis of Alzheimer's disease is hard, particularly at the early stage of the disease, mainly because symptoms are often dismissed as normal consequences of ageing. In addition, other pathologies (e.g. dementia with Lewy bodies, fronto-temporal dementia, and vascular dementia) share some symptoms with Alzheimer's disease at the early stage. To diagnose Alzheimer's disease, extensive tests are required to eliminate all other possible causes. These tests include comprehensive neuropsychological evaluations, neurological examination, blood tests, brain imaging techniques and spinal fluid analysis if needed [11]. Diagnosis of Alzheimer's disease by non-invasive and inexpensive techniques will allow dispensing better care to patients.

In the last years, the potential use of electroencephalography (EEG) for diagnosing dementia pathologies, and in particular Alzheimer's disease has been extensively investigated [12–19]. EEG is a non-invasive, relatively inexpensive, and potentially mobile technology with high temporal resolution (on the order of milliseconds). It was mainly investigated as a tool for AD diagnosis, by comparing EEG recordings of AD patients only to those of control subjects (healthy subjects) [12,13,15,17,18].

It is widely admitted that Alzheimer's disease leads to a reduction in the complexity of EEG signals and changes in EEG synchrony. These modifications in EEG recordings have been used as discriminative features for AD diagnosis. Several methods were developed for assessing the complexity of EEG signals. The correlation dimension and the first positive Lyapunov exponent were frequently used [20–25]. It was found that EEG signals from AD patients exhibit lower values of such measures (lower complexity) than signals from age-matched control subjects. Other information-theoretic methods, entropy-based approaches in particular, have emerged as potentially useful EEG markers of Alzheimer's disease: epoch-based entropy [26,27], sample entropy [28], Tsallis entropy [29], approximate entropy [30,31], multi-scale entropy [32], and Lempel-Ziv complexity [33]. These methods link the complexity of a signal to its unpredictability: irregular signals are more complex than regular ones since they are more unpredictable.

Since Alzheimer's disease is hypothesized to induce functional disconnection between brain regions, other studies focused on detecting the changes in the synchrony between pairs of EEG signals. A large variety of measures has been developed to quantify EEG synchrony: correlation coefficient [34], coherence [34–36], Granger causality [34,37], phase synchrony

[34,38,39], state space based synchrony [34,38,40], stochastic event synchrony [34,36,39,41,42] and mutual information [43]. All these studies reported decreased EEG synchrony in MCI and AD patients compared to healthy subjects.

To discriminate AD patients from healthy subjects, all the above-mentioned studies analyzed the EEG signals either in the time domain or in specific standard frequency bands: 0.1–4Hz (delta band), 4–8Hz (theta band), 8–12Hz (alpha band), 12–30Hz (beta band) and 30–100Hz (gamma band) [23,44], or in the whole frequency range between 4 and 30Hz [34]. Spectral analysis studies reported that Alzheimer's disease induces increased activity in the delta and theta frequency bands, as well as decreased activity in the alpha and beta bands [19,45–48]. Also, reduced spectral coherence between the two hemispheres was shown between alpha and beta frequency bands [14,49–52]. These spectral differences were also shown to be correlated with the severity of the disease [14,53,54]. Moreover, alpha rhythms are usually distributed in the occipital area for healthy subjects; in AD patients, they increasingly move towards anterior areas as the disease progresses [45,55,56]. Early stages of Alzheimer's disease have been associated with an increase of theta activity and/or a decrease of alpha activity. In more severe stages of Alzheimer's disease, an increase of both theta and delta activities has been observed together with a decrease of both alpha and beta activities, additionally to a reduction in the amplitude of the peak of alpha frequency band [57,58]. In all these studies, a 70%-85% correct detection rate is commonly achieved for different degrees of disease severity.

By contrast to all the above-mentioned investigations, the present study takes advantage of a database containing EEG data acquired from different patients in real clinical conditions. This database contains EEG data from patients with subjective cognitive impairment (SCI), possible AD patients (DSM IV definition), MCI patients and patients suffering from other pathologies, such as vascular dementia, psychosis, Lewy body dementia, and non neurodegenerative disorders (alcoholism, cerebral vascularitis, cerebellar abscess. . .). To the best of our knowledge, this is the first report of automatic discrimination, from EEG data, between SCI, MCI, and Mild to moderate possible AD patients. A similar work in the literature in terms of the exploited cohort is that of *Liedorp et al.* [59]. The authors used a large memory clinic database that contains EEG data of subjective memory complaints patients, MCI patients, AD patients, and patients with other dementias (psychiatric disorders, vascular dementia (VaD), fronto-temporal dementia, and Lewy bodies (DLB)). However, the authors investigated focal and diffuse abnormalities in different cognitive profiles of the database, based on a visual EEG assessment.

In the present work, both AD diagnosis and differential AD diagnosis are investigated. In the first case, possible AD patients are discriminated from SCI patients (AD diagnosis) only. In the second case, SCI patients and possible AD patients are discriminated from patients with MCI or other pathologies. The experiments involve the use of two features: an entropy-based complexity measure [26,27] and a synchrony measure [60,61], both computed in different frequency ranges and for different brain regions. The most relevant measures and the most relevant frequency range are selected with the Orthogonal Forward Regression (OFR) algorithm and the random probe method [62–64] to improve the accuracy of EEG classification using a Support Vector Machine classifier (SVM) [65,66].

Material and methods

Database description and pre-processing

The database was recorded in real clinical conditions between 2009 and 2013 at Charles-Foix Hospital (Ivry-sur-Seine, France). The EEG recordings were obtained at rest and with closed eyes using a Deltamed digital EEG acquisition system for a minimum of 20 minutes. Scalp electrodes were placed according to the modified International 10–20 system with 11 additional

electrodes in a common reference montage using a sampling rate of 256 Hz. Thirty electrodes were placed on the scalp (Fp1, Fp2, F7, F3, Fz, F4, F8, FT7, FC3, FC7, FC4, FT8, T3, C3, Cz, C4, T4, TP7, CP3, CPz, CP4, TP8, T5, P3, Pz, P4, T6, O1, Oz, O2).

The patients who complained of memory impairment were referred to the outpatient memory clinic of the Charles-Foix Hospital where they underwent a battery of tests for brain disorders, including neuropsychological test, brain imaging and blood samplings. Patients with epilepsy were excluded. Each patient was given a diagnosis at the memory clinic on the basis of the clinical, brain imaging, psychometric findings, and discussions held by a multidisciplinary medical team, using the standard diagnostic criteria: DSM-IV, NINDS, Jessen criteria for SCI, Mc Keith criteria for Lewy body dementia [2,3,67]. We didn't use EEG recordings to establish the diagnosis. This retrospective study was approved by the local ethical committee of the University Pierre and Marie Curie Paris 6. The database reflects what medical practitioners are facing in reality, as opposed to databases used in the literature [24,27,29,34–39] that are prone to experimental constraints that do not match the reality on the ground.

The database contains EEG data of 169 patients (mean age 75±11.2 years old, range 42–97 years old; 110 women). These patients are described in the Table 1.

For each subject, continuous epochs of 20 seconds, free from artifacts, were selected manually. They were then band-pass filtered with a third-order digital Butterworth filter between 1 and 30Hz.

Methodology

The purpose of this study is to develop a method that consists in: (i) discriminating automatically possible AD patients from patients who came to the hospital with cognitive complaint but with normal age-, gender -and education-adjusted performance on cognitive tests i.e. SCI patients (AD diagnosis); (ii) discriminating automatically possible AD patients from SCI patients and patients with MCI or other pathologies (differential AD diagnosis).

For AD diagnosis experiments, only two groups were considered: the 22 SCI patients and the 49 possible AD patients. For differential AD diagnosis, two cases were investigated. In the first case, three groups were considered: the first group contained the 22 SCI patients (SCI patients); the second group contained the 49 AD patients (AD patients), and the third group

Table 1. Clinical characteristics of the cohort. AD: Alzheimer's disease; aMCI: amnestic MCI; oMCI: other MCI; SCI: subjective cognitive impairment; BZD: benzodiazepine.

	SCI (n = 22)	MCI (n = 58)		AD (n = 49)		Other pathologies (n = 40)			
	SCI (n = 22)	aMCI (n = 6)	oMCI (n = 52)	AD (n = 28)	Mixed (n = 21)	Lewy body dementia (n = 3)	Psychosis (n = 13)	Vascular dementia (n = 9)	Non neuro-degenerative disorders (n = 15)
Age Years old (mean ±SD)	68.9±10.3	74.5±12.7	75.2±10.8	80.8±10.5	81.6± 7.3	76.0±6.1	64.1±12.5	79.3±6.3	70.1±11.1
Gender : female N (%)	18 (81,8%)	3 (50%)	32 (61,5%)	19 (67,8%)	11 (52,4%)	3 (100%)	11 (84,6%)	4 (44,4%)	9 (60%)
Education year									
MMSE (mean ±SD)	28.3±1.6	28.2±1.2	24.5±4.9	18.3±6.1	17.9±7.0	16±5.6	23.8±3.3	21.9±5.2	18.4±7.0
BZD use N (%)	4 (18.2%)	1 (16.7%)	5 (9.6%)	8 (28.6%)	9 (42.8%)	0	4 (30.8%)	2 (22.2%)	7 (46.7%)
Antidepressant use N (%)	2 (9%)	1 (16.7%)	10 (19.2%)	12 (42.8%)	13 (61.9%)	1 (33.3%)	4 (30.8%)	2 (22.2%)	6 (40%)
Neuroleptic use N (%)	0	0	2 (3.8%)	5 (17.8%)	3 (14.3%)	1 (33.3%)	1 (7.7%)	1 (11.1%)	3 (20%)
hypnotic use N (%)	5 (22.7%)	1 (16.7%)	12 (23.1%)	7 (25%)	6 (28.6%)	0	2 (15.4%)	0	5 (23.8%)

contained all the remaining 98 patients with MCI or other pathologies (Other patients). In the second case of differential AD diagnosis, additionally to the three groups defined in the latter case, a fourth group was defined by separating the 58 MCI patients (MCI patients) from the 40 patients with other pathologies (Other pathologies). Note that the "Other patients" group in the first case and "Other pathologies" group in the second case are heterogeneous and contain patients with variable EEG signatures.

The proposed method exploits two EEG features: epoch-based entropy, which is a measure of signal complexity, and bump models, which quantify the EEG local synchrony. Both features are computed in different brain regions and in the four EEG frequency bands. The most relevant brain regions and frequency ranges are selected with the Orthogonal Forward Regression (OFR) algorithm [63,64] using a leave-one-subject-out cross-validation procedure and the random probe method [62]. The selected features are subsequently fed to a polynomial SVM classifier [65,66].

EEG features

As mentioned above, epoch-based entropy and bump modeling were used for extracting relevant features from the EEG signal. These two measures have been reviewed earlier in [27,60]. A brief description is presented in the next two subsections.

Epoch-based entropy measure. Epoch-based entropy measure was introduced in [26,27] as a complexity measure for early screening of Alzheimer's disease. The reliability of this measure stems from the fact that it estimates the complexity of EEG signals not only locally over time (as classical complexity measures do), but also spatially by estimating the inter-channel complexity.

The measure is computed on piecewise stationary epochs of EEG signal using a Hidden Markov Model (HMM) [68], which performs a local density estimation at the epoch level. As in our previous studies [27], EEG signals are modeled by a continuous left-to-right HMM (Fig 1). The states of the HMM correspond to the stationary parts of the EEG signal, and the transitions of the HMM correspond to the variations of the signal. The EEG signal recorded from a given subject is thus considered as a succession of epochs, obtained by segmenting the signal by the Viterbi algorithm [68] using the corresponding subject's HMM. Thus, each obtained epoch corresponds to a state of the HMM and contains a given number of observations (sample points). For each epoch S_i, the probability density function is modeled by a mixture of M Gaussian functions; each multivariate Gaussian has a diagonal covariance matrix (Fig 1).

Then each observation z in a given epoch S_i is considered as a realization Z_i of a random variable Z that follows a given observation probability distribution $P_i(z)$ modeled by the Gaussian mixture. Consequently, each stationary epoch of the signal is associated to a random variable, and the entropy $H^*(Z_i)$ of the epoch S_i is that of an ensemble of realizations of Z_i:

$$H^*(Z_i) = -\sum_{z \in S_i} P_i(z).\log_2 P_i(z) \tag{1}$$

By averaging the entropy over the N epochs of the EEG signal of the subject, an entropy-based complexity value $EpEn(Z)$ of the signal, called "epoch-based entropy", is obtained as:

$$EpEn(Z) = \frac{1}{N}\sum_{i=1}^{N} H^*(Z_i) \tag{2}$$

To model the inter-relations between EEG time series recorded from D electrodes, an HMM is trained for each subject on a set of D EEG signals recorded from D electrodes. At
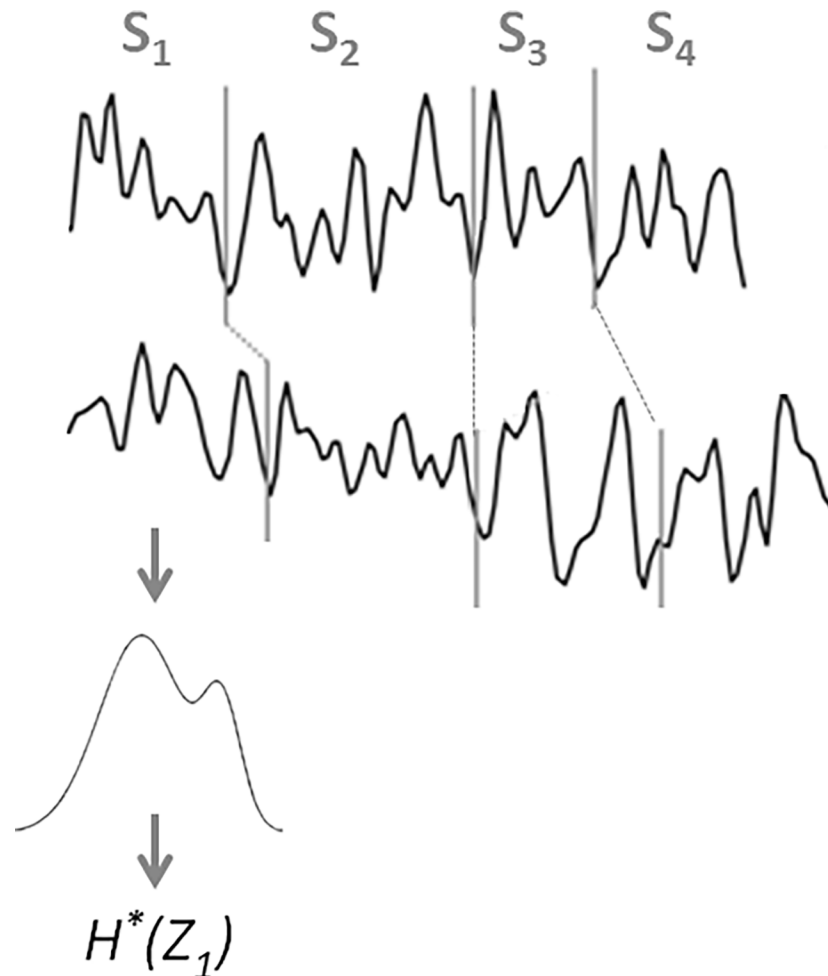
Fig 1. Illustration of multi-channel ($N = 4$, $D = 2$) EEG signal modeling with HMM.

https://doi.org/10.1371/journal.pone.0193607.g001

time t, a hidden state emits a D-dimensional observation vector. By applying the Viterbi algorithm, each EEG signal is segmented into N epochs, and the entropy $H^*(Z_i)$ of each epoch S_i is computed considering the probability density estimated by the HMM on the observations of the D epochs (Fig 1).

Although all N epochs are matched between EEG channels, the model does not constrain these epochs to be of equal length for all channels. Finally, by averaging the entropy over all the N epochs, an epoch-based entropy value associated to the multi-channel EEG of the subject is computed.

Bump models.   Signal features can be extracted from time-frequency maps by means of sparse bump models [60]; those models consist of time-frequency patterns ("bumps"), lasting roughly 4 time periods centered at a specific frequency. The bump modeling approach allows capturing oscillatory events in EEG on a trial-by-trial basis, which in turn may be considered as reliable characteristic signatures in Local Field Potentials and EEG signals [61]. Those patterns are likely to be representative of transient local synchronization of neuronal assemblies, conveying key information on high-order cognitive and sensory processing.

Wavelet time-frequency maps are computed using complex Morlet wavelets. The (continuous) wavelet transform $\mathbf{W}$ of a time series $\mathbf{x}$ is obtained as:

$$\mathbf{W}(k,s) \triangleq \sum_l \mathbf{x}(l)\Psi^*\left(\frac{l-k}{s}\right) \tag{3}$$

where $\Psi(k)$ is the mother' wavelet, s is a scaling factor, and * stands for complex conjugate. In this paper, we use the complex Morlet wavelet:

$$\Psi(k) = A.exp\left(\frac{-k^2}{2\sigma_t^2}\right).\exp(2i\pi f_0 k) \tag{4}$$

where σ_t^2 and f_0 jointly determine the number of oscillations in the wavelet. The complex Morlet wavelet family defined by $2i\pi f_0 k = 7$ results in the optimal resolution in time and frequency; it has also proven to be suitable for EEG signals [58].

Oscillatory events ("bumps") are extracted from the time-frequency maps using sparse bump modeling [69]. This procedure is described in more detail below.

Frequency-dependent z-score normalization [61,69] was applied to each trial:

$$z(f,t) = \frac{\mathbf{W}(f,t) - \mu_f}{\sigma_f} \tag{5}$$

where μ_f and σ_f are the mean and the standard deviation respectively of the wavelet map $\mathbf{W}$. The resulting z-score maps $z(f,t)$ are approximated by bump models z_{bumps}, which are sequences of basis functions b ("bumps") with parameters θ_k:

$$z(f,t) \approx z_{bumps}(\theta) = \sum_{k=1}^{N_b} b(\theta_k) \tag{6}$$

with $\theta = (\theta_1, \theta_2, \ldots, \theta_{N_b})$. This approximation retains the most salient oscillatory events in the z-scored map $z(f,t)$. As pointed out earlier, we hypothesize that those events are characteristic for EEG dynamics, and are therefore relevant for diagnosing Alzheimer's disease. In the present study, following [60,69], the basis functions $b(.)$ were half ellipsoids, and the parameters θ_k were vectors of five parameters: position in time and frequency, width in time and frequency, and amplitude.

Classification

Multi-class probabilistic SVM classifiers. This study involves a multi-class database containing four groups of patients: SCI patients, AD patients, MCI patients and patients with other pathologies. We are thus facing a K-class classification problem that was turned into a set of $K(K-1)/2$ two-class problems [70].

To distinguish between each pair of classes, a polynomial SVM classifier with a margin calibration is used to overcome the issue of unbalanced datasets [71]. Therefore $K(K-1)/2$ two-class SVM classifiers are trained in order to estimate pairwise posterior probabilities. The SVM outputs were mapped to posterior probabilities using Platt's estimation method [72]. The global probability that an observation (a patient) described by the

feature vector x, belongs to class C_i is computed as:

$$\Pr(C_i/\mathrm{x}) = 1 / \left(\sum_{\substack{j=1 \\ j \neq i}}^{K} \frac{1}{Pr_{ij}} - (K-2) \right) \tag{7}$$

where K is the number of classes and Pr_{ij} is the probability of the observation belonging to the class i, estimated by the SVM classifier separating class C_i from class C_j.

Feature selection. Epoch-based entropy and bump models features are computed on different frequency bands and on different brain regions. This leads to a large number of candidate input features to the SVM classifiers. Since the study also involves a multi-class problem, feature selection was performed to determine which features, among the candidate features, are the most relevant for discriminating each pair of classes. To rank the candidate features in order of decreasing relevance, we used the Orthogonal Forward Regression (OFR) algorithm [63,64] with a leave-one-subject-out cross-validation procedure, summarized as follows:

1. Select the candidate feature f_i that best correlates to the output to be modeled;

2. Project the output vector onto the null space of the selected feature. Orthogonalize the rest of features using Gram-Schmidt orthogonalization;

3. Remove the selected feature f_i from the list of candidate features;

4. Return to (1) until termination by the random probe method described below.

In order to select the features, we applied the random probe method [62]: 100 probes, i.e. random realizations of features, are generated, concatenated to the set of real data, and all features (real and probe) are ranked as described above. The user defines an acceptable risk that a feature might be kept although, given the available data, it might be less relevant than the probe. At each step of the selection procedure, the following steps are performed:

1. Obtain a candidate feature from OFR;

2. Estimate the value of the cumulative distribution function of the rank of the probe for the rank of the candidate feature. If the value is smaller than the acceptable risk, keep the feature and return to step 2 of OFR; otherwise, discard the considered feature and terminate the procedure.

Experimental results

For all 169 subjects, epoch-based entropy and bump models were computed in different frequency bands and for different brain regions. On the basis of the results reported in the literature on Alzheimer's disease detection with EEG, 16 features were considered as primary candidate variables: 7 features related to epoch-based entropy (*EpEn*) and 9 features related to bump models (BM), as reported in Table 2. The squared primary variables were considered as secondary variables in order to take into account possible non-linearities, so that the total number of candidate features was 32.

AD diagnosis

AD diagnosis consists in discriminating SCI subjects (22 in the database) from AD subjects (49 in the database). As mentioned above, 32 candidate features were computed for each

Table 2. The computed epoch-based entropy and bump model features for each subject.

Epoch-based entropy (*EpEn*)	Brain regions		
	All electrodes	Temporal (left and right)	Frontal+Occipital
Frequency range (Hz)	1–4 ; 4–8 ; 8–12 ; 12–30 ; 8–30	8–30	8–30
Bump models (*BM*)	Brain regions		
	Frontal	Occipital	Temporal (left and right)
Frequency range (Hz)	4–8 ; 8–12 ; 12–30	4–8 ; 8–12 ; 12–30	4–8 ; 8–12 ; 12–30

https://doi.org/10.1371/journal.pone.0193607.t002

subject. Feature selection was performed using OFR algorithm with a leave-one-subject-out cross-validation procedure, as described in Section 2.4.2. Random variables (probes) were added to the feature set and only variables that ranked better than 90% of the probe were kept for classification. Therefore, the selected features are, in order of decreasing relevance:

a) *EpEn* computed on all electrodes, in the [8–12] Hz band,

b) *EpEn* computed on the Temporal region, in the [8–30] Hz band,

c) *BM* computed on the Frontal region, in the [4–8] Hz band,

d) *EpEn* computed on all electrodes, in the [8–30] Hz band,

e) *EpEn* computed on the Frontal + Occipital region, in the [8–30] Hz band.

This result shows that almost all selected features are related to the complexity measure, namely Epoch-based entropy (*EpEn*). Also, the optimal range on which EEG signal is the most informative for AD screening is 8 to 30Hz (alpha and beta bands).

For further analysis, Fig 2 shows the box plots of features values obtained on SCI subjects and AD patients considering only the features that best discriminate these two groups. Fig 2A, Fig 2B, Fig 2D and Fig 2E show that AD patients have lower median values of epoch-based entropy than control subjects. This result is consistent with the literature: EEG signals from AD patients exhibit lower complexity values than age-matched control subjects in almost all channels [23,24,27,28]. In addition, Fig 2C indicates an increased EEG synchrony in the theta band for AD patients compared to SCI subjects. This result is consistent with previously published studies: AD induces an increased activity in the theta band [12,43,46]. It is interesting to point out that these results are still valid although the control subjects of this database are not healthy subjects since they have some memory complaints.

The selected features are subsequently used as inputs to a second-degree polynomial SVM classifier with soft margin. The performance of the SVM classifier was estimated by leave-one-subject-out cross-validation, which is known to provide an unbiased estimation of the generalization error [73]. Due to the small size of the database, the generalization error was not estimated on separate test data. Results of the classification showed that a correct classification rate of 91.6% is reached when discriminating SCI subjects from AD patients, with a specificity (proportion of well classified SCI patients) of 100% and a sensitivity (proportion of well classified AD patients) of 87.8%.

This result demonstrates the reliability of the used features and the proposed method for detecting Alzheimer's disease. The result also shows a very good detection of SCI subjects with a specificity of 100% despite the fact that SCI subjects are not totally healthy subjects since they have some memory complaints.
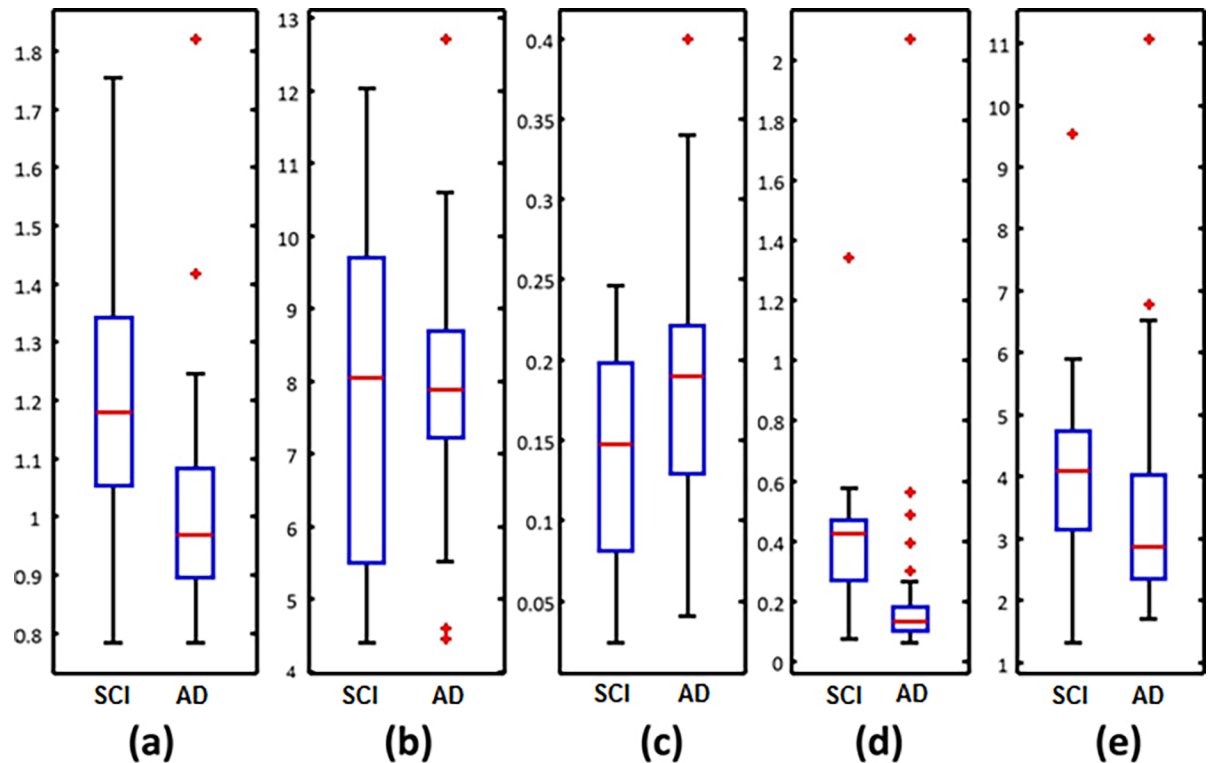
Fig 2. Box plots of the best features discriminating SCI patients from AD patients. The figures follow the ranking in order of decreasing relevance: (a) *EpEn* on all electrodes [8–12] Hz; (b) *EpEn* on temporal region [8–30] Hz; (c) BM on Frontal region [4–8] Hz; (d) *EpEn* on all electrodes [8–30] Hz; (e) *EpEn* on frontal + occipital region [8–30] Hz.

https://doi.org/10.1371/journal.pone.0193607.g002

Differential AD diagnosis with three groups of patients

For differential AD diagnosis, the 169 subjects of the database were first organized into three groups: group 1 contains the 22 SCI subjects, group 2 contains the 49 AD patients, and group 3 contains the other 98 patients (with MCI or other pathologies).

Feature selection was performed on the 32 candidate features described in Table 2, in order to find the most relevant features for pairwise discrimination of the three groups. Table 3 shows the selected features for discriminating SCI from AD patients, SCI from "Other" patients, and AD from "Other" patients. The superscript indicates the order of the feature as ranked by OFR ("a" corresponds to rank 1, "b" to rank 2, etc).

Table 3 shows that the majority of selected features are related to the complexity measure. Moreover, the optimal range on which EEG signal is more relevant for AD diagnosis is from 8 to 30Hz (alpha and beta bands).

Table 3. Best combination of features for discriminating SCI patients from AD patients (SCI vs. AD), SCI patients from those with MCI or other pathologies (SCI vs. Other), and AD patients from those with MCI or other pathologies (AD vs. Other).

Selected features	Epoch-based entropy			Bump Models	
	All electrodes	**Temporal (left and right)**	**Frontal + Occipital**	**Frontal**	**Temporal (left and right)**
SCI vs. AD	[8–12][a] [8–30][d]	[8–30][b]	[8–30][e]	[4–8][c]	-
SCI vs. Other	[8–12][a] [12–30][c]	-	[8–30][d]	[8–12][b]	[8–12][e]
AD vs. Other	[8–12][f] [12–30][d] [8–30][b]	[8–30][a]	[8–30][c]	[12–30][g]	[12–30][e]

[a-g] indicate the order of the feature as ranked by OFR ("a" corresponds to rank 1, "b" to rank 2, etc)

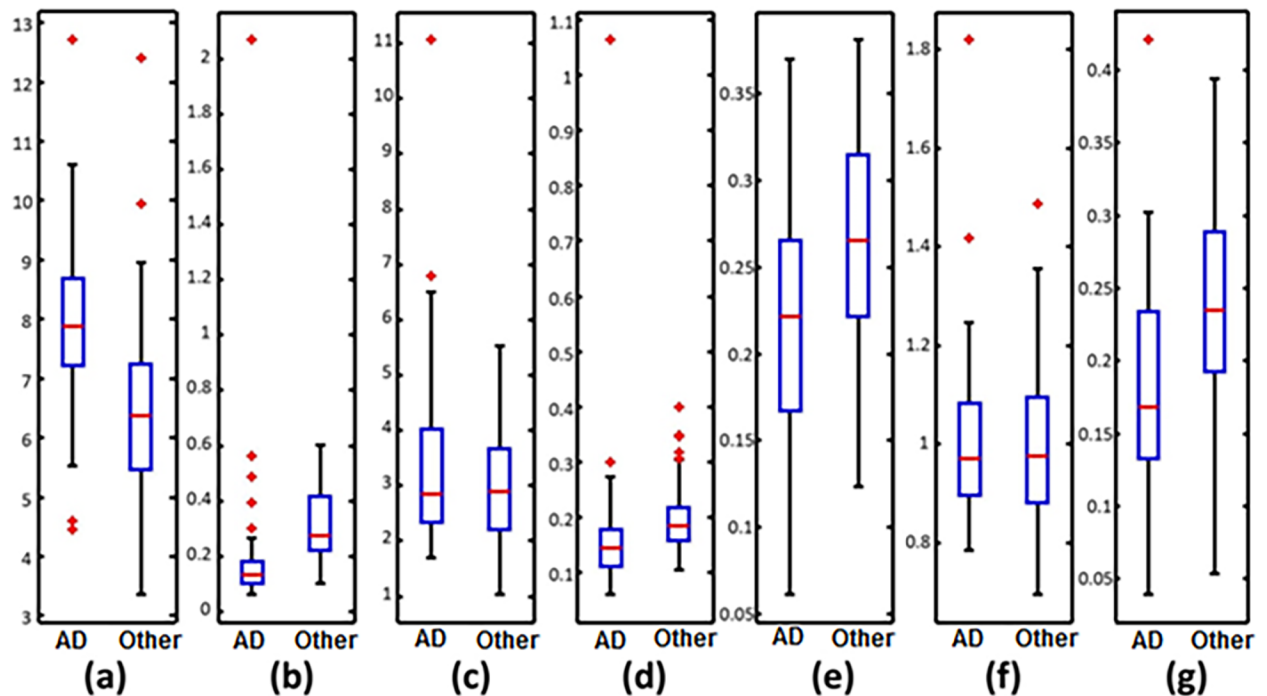https://doi.org/10.1371/journal.pone.0193607.t003

Fig 3. Box plots of the most relevant features for discriminating possible AD patients from "Other" patients (patients with MCI or other pathologies). Figures follow the same order given by the OFR algorithm as noted in Table 3: (a) *EpEn* on Temporal region [8–30] Hz; (b) *EpEn* on all electrodes [8–30] Hz; (c) *EpEn* on Frontal + Occipital region [8–30] Hz; (d) *EpEn* on all electrodes [12–30] Hz; (e) *BM* on Temporal region [12–30] Hz; (f) *EpEn* on all electrodes [8–12] Hz; (g) *BM* on Frontal region [12–30] Hz.

A larger number of features is necessary for discriminating AD from "Other" patients than for discriminating SCI from AD and SCI from "Other" patients. This fact reflects the difficulty of detecting AD patients from patients with pathologies that share symptoms with AD.

For further analysis, we present in Fig 3 the box plots of the 7 features values that best discriminate the 49 AD patients from the 98 patients with MCI or other pathologies.

Possible AD patients show a decreased EEG synchrony in the beta frequency range for both temporal (Fig 3E) and frontal (Fig 3G) regions. The Mann-Whitney test indicates that there is a significant difference ($p<0.001$) between the distribution of features of EEG signals of AD patients and the distribution of features of EEG signals of "Other" patients; this demonstrates the potential of the employed synchrony measure for detecting loss in EEG synchrony caused by Alzheimer's disease.

In terms of complexity values, two behaviors appear in the alpha and beta ranges depending on the brain region:

(i) For EEG channels of all brain regions (Fig 3B and Fig 3D), it clearly appears that Alzheimer's disease induces a reduction in complexity compared to the other pathologies. There is a significant difference ($p<$1e-6) between the distributions of features of the two populations;

(ii) For the temporal brain region (Fig 3A), EEG signals are more complex for AD patients than for the patients with MCI or other pathologies ($p<$1e-4).

The selected features are used as inputs of the corresponding three SVM classifiers associated to the three discriminations (SCI vs. AD, SCI vs. Other, AD vs. Other). The probabilistic outputs of the SVM classifiers are used to estimate the posterior probabilities of the classes

Table 4. Confusion matrix for differential AD diagnosis with three groups of patients.

Three groups	SCI patients	AD patients	Other patients
SCI patients	**81.8%**	0%	18.2%
AD patients	8.2%	**87.8%**	4.1%
Other patients	6.1%	5.1%	**88.8%**

https://doi.org/10.1371/journal.pone.0193607.t004

following the procedure described in section 2.4.1. The classification performances estimated by leave-one-subject-out cross-validation are presented in Table 4.

First, Table 4 shows that the proposed methodology leads to a high rate of correct classification of the subjects, higher than 82% (see the diagonal of the confusion matrix). Moreover, the detection rates are almost equivalent for the three groups (81.8% to 88.8%); this reflects the tradeoff made by our methodology between EEG specificity and EEG sensitivity for classifying the three groups.

Almost 82% of SCI patients are correctly detected, and no SCI patient (0%) was misclassified as AD patient. However, almost 18% of SCI patients were detected as patients with MCI or other pathologies. This result might be due to the fact that 59.2% of the 98 remaining patients of the database are MCI patients, which are very close to the SCI patients. This hypothesis is confirmed in section 3.3 below.

Table 4 also shows that 87.8% of AD patients are well detected. Among the remaining misclassified AD patients, two thirds are detected as SCI subjects (8.2%) and one third as suffering from MCI or other pathologies (4.1%). For the "Other" patients, 88.8% of them are well detected, and among the misclassified patients, half of them are considered as AD patients, the others as SCI patients.

For further analysis, we studied the effect of age on AD diagnosis as an etiological factor. To this end, we added age to the set of initial candidate variables and performed feature selection as described in Section 2.4.2. As a result, age was selected only for discrimination of SCI vs. AD, and not selected for SCI vs. Other and AD vs. Other, and the overall classification performance was found to decrease.

As a final test, the selected features for SCI vs. AD, without considering age in the set of initial candidates, were orthogonalized with respect to the vector of ages using Gram-Schmidt orthogonalization, thereby generating a new set of features that were decorrelated from age; these features were input to a new SVM classifier. The classification performance was found to be the same as obtained previously. This shows that the information on age present implicitly in the features had no influence on the classification results.

The results of the above two numerical experiments on age show that, for the differential diagnostics of interest in the present study, and given the available data, age is not a relevant factor.

Differential AD diagnosis with four groups of patients

In the present subsection, the group including patients with MCI and other pathologies is split into two distinct groups: "MCI" group and "Other pathologies" group. The same procedure was used as in Section 3.2: pairwise classification between the groups was performed by 6 SVM classifiers, after feature selection. The performance was estimated by leave-one-subject-out cross-validation.

The results showed that for discriminating the 6 pairs of groups, EEG analysis should be carried out on the frequency range of 4–30 Hz. In contrast to the previous sections, where, in almost all cases, only the alpha and beta ranges were taken into account, the theta band is

Table 5. Confusion matrix for differential AD diagnosis with four groups of patients.

Four groups	SCI	AD	MCI	Other pathologies
SCI	**81.8%**	0%	18.2%	0%
AD	6.1%	**89.8%**	2.0%	2.0%
MCI	5.2%	6.9%	**60.3%**	27.6%
Other pathologies	2.5%	5%	47.5%	**45%**

additionally considered. We also found that only one feature was selected for distinguishing MCI patients from the patients with other pathologies. This encourages the use of other features for better characterizing MCI patients.

The results of the classification of the four groups are shown in Table 5 in terms of confusion matrix. We first observe on the diagonal of the confusion matrix, that 82% of SCI patients and almost 90% of AD patients are well detected. However, we notice the difficulty in detecting MCI patients (60.4%) and patients with other pathologies (45%).

Moreover, the misclassified SCI patients are all classified as MCI patients. This result confirms our hypothesis stated in Section 3.2: SCI patients in the database suffer from memory complaints, which makes them similar to MCI patients based on our EEG descriptors. This result is particularly interesting in the framework of AD diagnosis, since this is the first EEG study, to the best of our knowledge, where SCI patients are discriminated from MCI and Mild AD patients: usually, MCI and Mild AD patients are discriminated from healthy subjects.

The results show that the present features are not very efficient for discriminating MCI patients from patients with other pathologies: only 60.3% of MCI patients are well detected, and among the misclassified MCI, 70% of them are considered as patients with other pathologies.

Since these four groups contain mixed patients with different impairments, we report in Table 6 the distribution of the misclassified patients in each group to give insight into the results.

When analyzing the distribution of the misclassified patients in Table 6, we observe that:

a) the only AD patient associated to "Other pathologies" group has a mixed AD (AD with other pathology).

b) the 5 misclassified aMCI patients (among the 6 existing in the database) are associated to AD group and "Other pathologies" group. This result comforts the fact that amnestic form of MCI predicts the progression to neurodegenerative disease.

c) three misclassified MCI patients are associated to SCI group and two others are associated to AD group and "Other pathologies" group. Compared to amnestic MCI, the other forms of MCI are more confused with SCI subjects.

d) among the 21 misclassified patients from "Other pathologies" group, 19 patients are considered as MCI patients. The only patient from "Other pathologies" group considered as SCI subject has a vascular dementia. Also, two patients with Lewy body dementia

Table 6. Distribution of the misclassified patients in the four groups. Refer to Table 1 that describes the cohort in details.

	SCI	MCI	AD	Other pathologies
Among the 49 patients of AD group: 5 are misclassified	2 AD 1 mixed AD	1 AD	/	1 mixed AD
Among the 58 patients of MCI group: 23 are misclassified	3 MCI	/	3 aMCI 1 MCI	2 aMCI 14 MCI
Among the 40 patients with Other pathologies: 22 are misclassified	1 vascular	5 vascular 9 non disorder 5 psychosis	2 Lewy	/

(among the 3 existing in the database) are considered as AD patients. This result reflects that our selected features couldn't differentiate between Alzheimer's dementia and Lewy body dementia.

Discussion and conclusion

In clinical practice, medical doctors have to discriminate patients suffering from Alzheimer's disease from persons suffering from other types of dementia, or MCI, or from patients with subjective cognitive impairment. Alzheimer's disease (AD) is consequently sometimes difficult to diagnose and discriminate from these pathologies, without using cerebrospinal fluid (CSF) biomarkers or single-photon emission computerized tomography (SPECT-scan).

Misdiagnosed patients suffer from unsuitable medical care, and have a societal cost. For instance, patients suffering from vascular dementia with prior AD diagnosis use substantially more medical services every year until their dementia diagnosis, resulting in incremental annual medical costs of approximately $9,500-$14,000 [74].

It is widely admitted that EEG is potentially very useful for AD diagnosis. Nevertheless, state-of-the-art publications have three limitations. First, most publications report studies conducted on small databases, of around 20 persons, containing EEG signals from only age-matched healthy subjects and from patients affected by Alzheimer's disease. Second, the methods advocated for EEG-based AD diagnosis tend to have low specificity, hence poor detection of healthy subjects [58,75]. Third, for all these studies, the accuracy of AD diagnosis is not evaluated in a differential diagnosis context with respect to other pathologies.

The present study overcomes the above limitations, by analyzing a large database containing EEG data recorded in different pathologies, in real clinical conditions. In addition to AD and MCI patients, we considered patients with different pathologies, and SCI patients who joined the study with a suspicion of neurodegenerative disorder, but were diagnosed as not suffering from any objective cognitive deficit. To the best of our knowledge, no study so far has been carried out on AD diagnosis in a differential diagnosis context based on an automatic discrimination from EEG data.

In our framework, two tasks were performed in the present study: (i) discriminating AD patients from SCI patients (AD diagnosis); (ii) discriminating AD patients from patients affected by other pathologies (differential AD diagnosis). Based on measures of synchrony and complexity, we discriminated AD patients from SCI patients with high specificity, and discriminated AD patients from patients with other pathologies. The classifiers are Support Vector Machines, with feature selection by the random probe method; performance estimation is performed by leave-one-subject-out cross-validation.

We obtained a high accuracy for the classification of SCI vs. AD patients (91.6% accuracy, 100% specificity and 87.8% sensitivity). To the best of our knowledge, this is the first report of AD vs. SCI automatic classification based on EEG analysis. Knowing that the only reliable AD diagnosis is achieved by a post-mortem analysis of the brain [9], a reasonable goal was to reach an 85~90% accuracy. Recent scientific studies in the field of AD diagnosis reported high accuracy in classification tasks comparing AD patients and aged-matched healthy controls [12,13,15,17,18,24,27]. Our results are in the same order of accuracy as these studies–despite the fact that SCI patients, as opposed to control healthy subjects, may suffer from biological degradations [76,77].

In addition, by discriminating AD, SCI and Other patients including MCI, we showed that the classification accuracies remained similar for a three-group classification (81.8% to 88.8% accuracies). Thus our method provides a good tradeoff between specificity and sensitivity for the three groups. When analyzing the selected features for classification, our study reveals that

Alzheimer's disease induces a reduction of EEG complexity and an increase of EEG synchrony in the theta band, compared to SCI patients, considered in this work as control subjects. This is important, since it shows that the results of the literature on AD screening remain valid when comparing AD patients to SCI patients.

Finally, when splitting the "Other" group into "MCI" group and "Other pathologies" group (Section 3.3), all misclassified SCI patients were classified as MCI, which might be the consequence of the similarities between SCI patients and MCI patients: it has been shown that a proportion of SCI patients are actually at an early stage of MCI [78]. MCI patients were not correctly classified against patients with other pathologies. It is not very surprising that we failed to classify properly all these pathologies from the MCI stage, which could be caused by several different underlying mechanisms. Moreover, there would be a large overlap between the EEG signatures of these two groups due to causal heterogeneity in the "Other pathologies" group. A larger database would probably be necessary and other EEG features should be investigated.

In future work, we will focus the study of differential AD diagnosis on MCI patients in order to recover the best descriptors of this group of patients. We will also apply the methodology described in this paper on the other EEG data collected at Charles-Foix hospital to study the effectiveness of our method to discriminate, in blind manner, the different groups of patients.

Acknowledgments

Author Contributions

Conceptualization: Nesma Houmani, François Vialatte, Gérard Dreyfus, Vi-Huong Nguyen-Michel, Jean Mariani, Kiyoka Kinugawa.

Data curation: Vi-Huong Nguyen-Michel, Jean Mariani, Kiyoka Kinugawa.

Formal analysis: Nesma Houmani, François Vialatte, Esteve Gallego-Jutglà, Gérard Dreyfus, Kiyoka Kinugawa.

Funding acquisition: François Vialatte, Jean Mariani, Kiyoka Kinugawa.

Investigation: Nesma Houmani, Esteve Gallego-Jutglà.

Methodology: Nesma Houmani, François Vialatte, Gérard Dreyfus, Kiyoka Kinugawa.

Project administration: François Vialatte, Jean Mariani, Kiyoka Kinugawa.

Resources: François Vialatte, Jean Mariani.

Software: Nesma Houmani, François Vialatte, Esteve Gallego-Jutglà.

Supervision: Nesma Houmani, François Vialatte, Gérard Dreyfus, Jean Mariani, Kiyoka Kinugawa.

Validation: Nesma Houmani, François Vialatte, Gérard Dreyfus.

Visualization: Nesma Houmani, François Vialatte.

Writing – original draft: Nesma Houmani, François Vialatte, Gérard Dreyfus, Jean Mariani, Kiyoka Kinugawa.

Writing – review & editing: Nesma Houmani, François Vialatte, Gérard Dreyfus, Jean Mariani, Kiyoka Kinugawa.

References

1. World Alzheimer Report 2015. The Global Impact of Dementia: An analysis of prevalence, incidence, cost and trends. Alzheimer's disease International. 2015.

2. Jessen F, Amariglio RE, Van Boxtel M, Breteler M, Ceccaldi M, Chételat F, et al. A conceptual framework for research on subjective cognitive decline in preclinical Alzheimer's disease. Alzheimers Dementia. 2014; 10(6): 844–52. https://doi.org/10.1016/j.jalz.2014.01.001

3. Mitchell AJ, Beaumont H, Ferguson D, Yadegarfar M, Stubbs B. Risk of dementia and mild cognitive impairment in older people with subjective memory complaints: meta-analysis. Acta Psychiatrica Scandinavica, 2014; 130(6):349–51. https://doi.org/10.1111/acps.12336

4. Petersen RC, Roberts RO, Knopman DS, Boeve BF, Geda YE, Ivnik RJ, et al. Mild cognitive impairment: ten years later. Arch. Neurology. 2009; 66(12): 1447–55. https://doi.org/10.1001/archneurol.2009.266

5. Weiner MW, Veitch DP, Aisen PS, Beckett LA, Cairns NJ, Green RC, et al. The Alzheimer's disease neuroimaging initiative: a review of papers published since its inception. Alzheimer's Dement. 2012; 8 (1 Suppl): S1–68. https://doi.org/10.1016/j.jalz.2011.09.172

6. Alzheimer's Association Report. 2014 Alzheimer's disease facts and figures. Alzheimer's and Dementia. 2015.

7. Bracco L, Gallato R, Grigoletto F, Lippi A, Lepore V, Bino G, et al. Factors affecting course and survival in Alzheimer's disease: a 9-years longitudinal study. Arch Neurol. 1994; 51(12): 1213–9. PMID: 7986176

8. Helzner EP, Scarmeas N, Cosentino S, Tang MX, Schupf N, Stern Y. Survival in Alzheimer disease: a multiethnic, population-based study of incident cases. Neurology. 2008; 71(19): 1489–95. https://doi.org/10.1212/01.wnl.0000334278.11022.42 PMID: 18981370

9. Cummings J, Aisen PS, Dubois B, Frölich L, Jack CR Jr, Jones RW, et al. Drug development in Alzheimer's disease: the path to 2025. Alzheimer's Research & Therapy. 2016; 8:39. https://doi.org/10.1186/s13195-016-0207-9

10. Scheltens P, Blennow K, Breteler MM, de Strooper B, Frisoni GB, Salloway S, et al. Alzheimer's disease. The Lancet. 2016; 388(10043): 505–17. https://doi.org/10.1016/S0140-6736(15)01124-1

11. Palmer K, Berger AK, Monastero R, Winblad B, Bäckman L, Fratiglioni L. Predictors of progression from mild cognitive impairment to Alzheimer disease. Neurology. 2007; 68(19):1596–602. https://doi.org/10.1212/01.wnl.0000260968.92345.3f PMID: 17485646

12. Dauwels J, Srinivasan K, Reddy MR, Musha T, Vialatte FB, Latchoumane C, et al. Slowing and Loss of Complexity in Alzheimer's EEG: Two Sides of the Same Coin? International Journal of Alzheimer's Disease. 2011. Vol. 2011, Article ID 539621, 10 pages. https://doi.org/10.4061/2011/539621

13. Alberdi A, Aztiria A, Basarab A. On the early diagnosis of Alzheimer's disease from multimodal signals: A survey. Artificial Intelligence in Medicine. 2016; 71:1–29. https://doi.org/10.1016/j.artmed.2016.06.003 PMID: 27506128

14. Besthorn C, Förstl H, Geiger-Kabisch C, Sattel H, Gasser T, Schreiter-Gasser U. EEG coherence in Alzheimer disease. Electroencephalography and Clinical Neurophysiology. 1994; 90(3): 242–5. PMID: 7511505

15. Dauwels J, Vialatte FB, Cichocki A. Diagnosis of Alzheimer's disease from EEG signals: where are we standing? Current Alzheimer Research. 2010; 7(6): 487–505. PMID: 20455865

16. Leuchter AF, Cook IA, Newton TF, Dunkin J, Walter DO, Rosenberg-Thompson S, et al. Regional differences in brain electrical activity in dementia: use of spectral power and spectral ratio measures. Electroencephalography and Clinical Neurophysiology. 1993; 87(6):385–393. https://doi.org/10.1016/0013-4694(93)90152-L. PMID: 7508371

17. Malek N, Baker MR, Mann C, Greene J. Electroencephalographic markers in dementia. Acta Neurologica Scandinavica. 2017; 135(4):388–393. https://doi.org/10.1111/ane.12638 PMID: 27430350

18. Vecchio F, Babiloni C, Lizio R, Fallani Fde V, Blinowska K, Verrienti G, et al. Resting state cortical EEG rhythms in Alzheimer's disease: toward EEG markers for clinical applications: a review. Supplements to Clinical Neurophysiology. 2013; 62: 223–236. https://doi.org/10.1016/B978-0-7020-5307-8.00015-6. PMID: 24053043

19. Gouw AA, Alsema AM, Tijms BM, Borta A, Scheltens P, Stam CJ, et al. EEG spectral analysis as a putative early prognostic biomarker in nondemented, amyloid positive subjects. Neurobiology of Aging. 2017; 57: 133–142. https://doi.org/10.1016/j.neurobiolaging.2017.05.017 PMID: 28646686

20. Adeli H, Ghosh-Dastidar S, Dadmehr N. Alzheimer's disease: models of computation and analysis of EEGs. Clinical and EEG Neuroscience. 2005; 36(3):131–140. https://doi.org/10.1177/155005940503600303

21. Jelles B, van Birgelen JH, Slaets JP, Hekster RE, Jonkman EJ, Stam CJ. Decrease of nonlinear structure in the EEG of Alzheimer patients compared to healthy controls. Clinical Neurophysiology. 1999; 110(7): 1159–1167. https://doi.org/10.1016/S1388-2457(99)00013-9. PMID: 10423182

22. Jeong J, Kim SY, Han SH. Non-linear dynamical analysis of the EEG in Alzheimer's disease with optimal embedding dimension. Electroencephalography and clinical Neurophysiology. 1998; 106(3): 220–228. https://doi.org/10.1016/S0013-4694(97)00079-5 PMID: 9743280

23. Jeong J, Chae JH, Kim SY, Han SH. Nonlinear dynamic analysis of the EEG in patients with Alzheimer's disease and vascular dementia. Journal of Clinical Neurophysiology 2001; 18(1): 58–67. PMID: 11290940

24. Takahashi T. Complexity of spontaneous brain activity in mental disorders. Progress in Neuro-psychopharmacology & Biological Psychiatry. 2013; 45: 258–266. https://doi.org/10.1016/j.pnpbp.2012.05.001

25. Yagyu T, Wackermann J, Shigeta M, Jelic V, Kinoshita T, Kochi K, et al. Global dimensional complexity of multichannel EEG in mild Alzheimer's disease and age-matched cohorts. Dement Geriatr. Cogn. 1997; 8(6): 343–347. https://doi.org/10.1159/000106653

26. Houmani N, Vialatte FB, Latchoumane C, Jeong J, Dreyfus G. Stationary Epoch-based Entropy Estimation for Early Diagnosis of Alzheimer's Disease. 12th Low Voltage Low Power Conference. IEEE FTFC 2013. 1–4. Paris, France. 2013.

27. Houmani N, Vialatte FB, Dreyfus G. Epoch-based Entropy for Early Screening of Alzheimer's Disease. International Journal of Neural Systems. 2015; 25(8): 1550032. https://doi.org/10.1142/S012906571550032X PMID: 26560459

28. Abásolo D, Hornero R, Espino P, Alvarez D, Poza J. Entropy analysis of the EEG background activity in Alzheimer's disease patients. Physiological Measurement. 2006; 27(3): 241–253. https://doi.org/10.1088/0967-3334/27/3/003 PMID: 16462011

29. De Bock T, Das S, Mohsin M, Munro NB, Hively LM, Jiang Y, et al. Early detection of Alzheimer's disease using nonlinear analysis of EEG via Tsallis entropy. Biomedical Sciences and Engineering Conference. 2010; 1–4. https://doi.org/10.1109/BSEC.2010.5510813

30. Abásolo D, Hornero R, Espino P, Poza J, Sánchez CI, de la Rosa R. Analysis of regularity in the EEG background activity of Alzheimer's disease patients with approximate entropy. Clinical Neurophysiology. 2005; 116(8): 1826–1834. https://doi.org/10.1016/j.clinph.2005.04.001 PMID: 15979403

31. Pincus SM. Approximate entropy as a measure of irregularity for psychiatric serial metrics. Bipolar Disorders. 2006; 8(5): 430–440. https://doi.org/10.1111/j.1399-5618.2006.00375.x

32. Escudero J, Abásolo D, Hornero R, Espino P, López M. Analysis of electroencephalograms in Alzheimer's disease patients with multiscale entropy. Physiological Measurement. 2006; 27(11): 1091–1106. https://doi.org/10.1088/0967-3334/27/11/004 PMID: 17028404

33. Abásolo D, Hornero R, Gómez C, García M, López M. Analysis of EEG background activity in Alzheimer's disease patients with Lempel-Ziv complexity and Central Tendency Measure. Medical Engineering & Physics. 2006; 28(4): 315–322. https://doi.org/10.1016/j.medengphy.2005.07.004

34. Dauwels J, Vialatte FB, Musha T, Cichocki A. A comparative study of synchrony measures for the early diagnosis of Alzheimer's disease based on EEG. NeuroImage. 2010; 49(1): 668–693. https://doi.org/10.1016/j.neuroimage.2009.06.056 PMID: 19573607

35. Escudero J, Sanei S, Jarchi D, Abásolo D, Hornero R. Regional coherence evaluation in mild cognitive impairment and Alzheimer's disease based on adaptively extracted magnetoencephalogram rhythms. Physiological Measurement. 2011; 32(8): 1163–1180. https://doi.org/10.1088/0967-3334/32/8/011 PMID: 21709337

36. Sankari Z, Adeli H, Adeli A. Wavelet coherence model for diagnosis of Alzheimer's disease. Clinical EEG and Neuroscience. 2012; 43(4): 268–278. https://doi.org/10.1177/1550059412444970 PMID: 22715491

37. Babiloni C, Pievani M, Vecchio F, Geroldi C, Eusebi F, Fracassi C, et al. White-matter lesions along the cholinergic tracts are related to cortical sources of EEG rhythms in amnesic mild cognitive impairment. Human Brain Mapping. 2009; 30(5):1431–1443. https://doi.org/10.1002/hbm.20612 PMID: 19097164

38. Czigler B, Csikós D, Hidasi Z, Anna Gaál Z, Csibri E, Kiss E, et al. Quantitative EEG in early Alzheimer's disease patients—power spectrum and complexity features. International Journal of Psychophysiology. 2008; 68(1):75–80. https://doi.org/10.1016/j.ijpsycho.2007.11.002 PMID: 18093675

39. Park YM, Che HJ, Im CH, Jung HT, Bae SM, Lee SH. Decreased EEG synchronization and its correlation with symptom severity in Alzheimer's disease. Neuroscience Research. 2008; 62(2):112–117. https://doi.org/10.1016/j.neures.2008.06.009 PMID: 18672010

40. Kramer MA, Chang FL, Cohen ME, Hudson D, Szeri AJ. Synchronization measures of the scalp EEG can discriminate healthy from Alzheimer's subjects. International Journal of Neural Systems. 2007; 17 (2): 61–69. https://doi.org/10.1142/S0129065707000932 PMID: 17565502

41. Dauwels J, Vialatte FB, Weber T, Cichocki A. Quantifying statistical interdependence by message passing on graphs, Part I: one-dimensional point processes. Neural Computation. 2009; 21(8): 2152–2202. PMID: 19670479

42. Dauwels J, Vialatte FB, Weber T, Musha T, Cichocki A. Quantifying statistical interdependence by message passing on graphs, Part II: multi-dimensional point processes. Neural Computation. 2009; 21(8): 2203–2268. https://doi.org/10.1162/neco.2009.11-08-899 PMID: 19409054

43. Jeong J, Gore JC, Peterson BS. Mutual information analysis of the EEG in patients with Alzheimer's disease. Clinical Neurophysiology. 2001; 112(5):827–835. PMID: 11336898

44. Kropotov JD. Quantitative EEG, Event-Related Potentials and Neurotherapy. Academic press. San Diego, California. 2009. ISBN: 978-0-12-374512-5.

45. Babiloni C, Ferri R, Moretti DV, Strambi A, Binetti G, Dal Forno G, et al. Abnormal fronto-parietal coupling of brain rhythms in mild Alzheimer's disease: a multicentric EEG study. The European Journal of Neuroscience. 2004; 19(9): 2583–2590. https://doi.org/10.1111/j.0953-816X.2004.03333.x PMID: 15128412

46. Cibils D. Dementia and qEEG (Alzheimer's disease). Supplements to Clinical Neurophysiology. 2002; 54: 289–294. https://doi.org/10.1016/S1567-424X(09)70463-5.

47. Jelic V, Shigeta M, Julin P, Almkvist O, Winblad B, Wahlund LO. Quantitative electroencephalography power and coherence in Alzheimer's disease and mild cognitive impairment. Dementia. 1996; 7(6): 314–323. PMID: 8915037

48. Nunez PL, Srinivasan R. Electric Fields of the Brain: the Neurophysics of EEG. Oxford: Oxford University. 2006.

49. Dunkin JJ, Leuchter AF, Newton TF, Cook IA. Reduced EEG coherence in dementia: state or trait marker? Biological Psychiatry. 1994; 35(11): 870–879. http://dx.doi.org/10.1016/0006-3223(94)90023-X. PMID: 8054410

50. Jeong J. EEG dynamics in patients with Alzheimer's disease. Clinical Neurophysiology. 2004; 115(7): 1490–1505. https://doi.org/10.1016/j.clinph.2004.01.001

51. Leuchter AF, Spar JE, Walter DO, Weiner H. Electroencephalographic spectra and coherence in the diagnosis of Alzheimer's-type and multi-infarct dementia: a pilot study. Archives of General Psychiatry. 1987; 44(11): 993–998. PMID: 3314770

52. Locatelli T, Cursi M, Liberati D, Franceschi M, Comi G. EEG coherence in Alzheimer's disease. Electroencephalography and Clinical Neurophysiology. 1998; 106(3): 229–237. PMID: 9743281

53. Hughes JR, Shanmugham S, Wetzel LC, Bellur S, Hughes CA. The relationship between EEG changes and cognitive functions in dementia: a study in a VA population. Clinical Electroencephalography. 1989; 20(2): 77–85. PMID: 2706793

54. Sloan EP, Fenton GW, Kennedy NS, MacLennan JM. Neurophysiology and SPECT cerebral blood flow patterns in dementia. Electroencephalography and Clinical Neurophysiology. 1994; 91(3): 163–170. PMID: 7522145

55. Claus JJ, Ongerboer de Visser BW, Walstra GJ, Hijdra A, Verbeeten B Jr, van Gool WA. Quantitative spectral electroencephalography in predicting survival in patients with early Alzheimer disease. Archives of Neurology. 1998; 55(8):1105–1111. PMID: 9708961

56. Kowalski JW, Gawel M, Pfeffer A, Barcikowska M. The diagnostic value of EEG in Alzheimer disease: correlation with the severity of mental impairment. Journal of Clinical. Neurophysiology. 2001; 18(6): 570–575. PMID: 11779971

57. Ihl R, Dierks T, Martin EM, Froölich L, Maurer K. Topography of the maximum of the amplitude of EEG frequency bands in dementia of the Alzheimer type. Biological Psychiatry. 1996; 39(5):319–325. http://dx.doi.org/10.1016/0006-3223(95)00174-3 PMID: 8704062

58. Vialatte FB, Dauwels J, Maurice M, Musha T, Cichocki A. Improving the Specificity of EEG for Diagnosing Alzheimer's Disease. International Journal of Alzheimer's Disease. 2011; 2011: 259069. https://doi.org/10.4061/2011/259069 PMID: 21660242

59. Liedorp M, van der Flier WM, Hoogervorst EL, Scheltens P, Stam CJ. Associations between patterns of EEG abnormalities and diagnosis in a large memory clinic cohort. Dementia and Geriatric Cognitive Disorders. 2009; 27(1):18–23. https://doi.org/10.1159/000182422 PMID: 19088474

60. Vialatte FB, Martin C, Dubois R, Haddad J, Quenet B, Gervais R, et al. A machine learning approach to the analysis of time-frequency maps, and its application to neural dynamics. Neural Networks. 2007; 20 (2): 194–209. https://doi.org/10.1016/j.neunet.2006.09.013 PMID: 17145165

61. Vialatte FB, Solé-Casals J, Dauwels J, Maurice M, Cichocki A. Bump time-frequency toolbox: a toolbox for time-frequency oscillatory bursts extraction in electrophysiological signals. BMC neuroscience. 2009; 10:46. https://doi.org/10.1186/1471-2202-10-46 PMID: 19432999

62. Stoppiglia H, Dreyfus G, Dubois R, Oussar Y. Ranking a random feature for variable and feature selection. Journal of Machine Learning Research. 2003; 3:1399–1414.

63. Chen S, Billings SA, Luo W. Orthogonal least squares methods and their application to nonlinear system identification. International Journal of Control. 1989; 50:1873–1896. https://doi.org/10.1080/00207178908953472.

64. Dreyfus G. Neural Networks: methodology and applications. Springer, 2005.

65. Campbell C, Yiming Y. Learning with Support Vector Machines. Morgan and Claypool Publisher Synthesis Lectures on Artificial Intelligence and Machine Learning. 2011.

66. Boser BE, Guyon IM, Vapnik VN. A training algorithm for optimal margin classifiers. Proceedings of the fifth annual workshop on Computational learning theory. 1992; 144–152.

67. McKeith IG, Dickson DW, Lowe J, Emre M, O'Brien JT, Feldman H, et al. Diagnosis and management of dementia with Lewy bodies. Third report of the DLB consortium. Neurology 2005; 65(12): 1863–1872. https://doi.org/10.1212/01.wnl.0000187889.17253.b1 PMID: 16237129

68. Rabiner LR, Juang BH. An introduction to hidden Markov models. IEEE ASSP Magazine. 1986.

69. Vialatte FB, Solé-Casals J, Dauwels J, Maurice M, Cichocki A. Bump Time Frequency toolbox software, version 1.0. 2008. Available at: http://www.bsp.brain.riken.jp/~fvialatte/bumptoolbox/download.html

70. Knerr S, Personnaz L, Dreyfus G. Single-layer Learning Revisited: a Stepwise Procedure for Building and Training a Neural Network. Neurocomputing: Algorithms, Architectures and Applications, vol: F68 of NATO ASI Series, Springer-Verlag. 1990.

71. Yang CY, Yang JS, Wang JJ. Margin calibration in SVM class-imbalanced learning. Neurocomputing 2009; 73:397–411. https://doi.org/10.1016/j.neucom.2009.08.006

72. Platt J. Probabilistic outputs for support vector machines and comparison to regularized likelihood methods. Advances in Large Margin Classifiers. 1999; 61–74.

73. Vapnik V. Statistical Learning Theory. Wiley, New York. 1998.

74. Hunter CA, Kirson NY, Desai U, Cummings AK, Faries DE, Birnbaum HG. Medical costs of Alzheimer's disease misdiagnosis among US Medicare beneficiaries. Alzheimer's and Dementia. 2015; 11(8): 887–895. https://doi.org/10.1016/j.jalz.2015.06.1889 PMID: 26206626

75. Scinto LFM, Daffner KR. Early Diagnosis of Alzheimer's Disease. Humana Press. Totowa, NJ, USA. 2000.

76. Ivanoiu A, Dricot L, Gilis N, Grandin C, Lhommel R, Quenon L, et al. Classification of non-demented patients attending a memory clinic using the new diagnostic criteria for Alzheimer's disease with disease-related biomarkers. Journal of Alzheimer's Disease. 2015; 43(3): 835–847. https://doi.org/10.3233/JAD-140651 PMID: 25114071

77. Sambuchi N, Muraccioli I, Alescio-Lautier B, Paban V, Sambuc R, Jouve É, et al. Subjective cognitive impairment and Alzheimer's disease: a two year follow up of 51 subjects during two years. Geriatrie et Psychologie Neuropsychiatrie du Vieillissement. 2015; 13(4): 462–471. https://doi.org/10.1684/pnv.2015.0575 PMID: 26707564

78. Wurtman R. Biomarkers in the diagnosis and management of Alzheimer's disease. Metabolism. 2015; 64 (3 Suppl 1): S47–50. https://doi.org/10.1016/j.metabol.2014.10.034